

Constructing Virtual IoT Network Topologies with a Brain-Inspired Connectivity Model

Masaya Murakami
Grad. School of Information
Science & Technology
Osaka University, Japan
m-murakami@ist.osaka-
u.ac.jp

Kenji Leibnitz
Center for Information and
Neural Networks
NICT & Osaka University,
Japan
leibnitz@nict.go.jp

Daichi Kominami
Graduate School of
Economics
Osaka University, Japan
d-kominami@econ.osaka-
u.ac.jp

Tetsuya Shimokawa
Graduate School of Frontier
Biosciences
Osaka University, Japan
shimokawa@fbs.osaka-u.ac.jp

Masayuki Murata
Grad. School of Information
Science & Technology
Osaka University, Japan
murata@ist.osaka-u.ac.jp

ABSTRACT

Wireless sensor networks will be one of the fundamental technologies for realizing the future *Internet of Things* (IoT) environment. In IoT, the number of connected devices is expected to increase drastically and there will be a wide variety of requirements for application services, which will lead to frequent modifications or construction/destruction of topologies. In such situations, it is essential to know how power-saving, low-latency, and highly efficient IoT network topologies can be constructed. In this paper, we take inspiration from the brain's network of interconnecting neurons is known for its efficient properties. We propose a virtual IoT network construction method based on the *Exponential Distance Rule* (EDR) model that describes the connection structure of the areas in the cerebral cortex. Since the original EDR model deals with large-scale networks with an enormous number of neurons and generates links between nodes considering physical distance constraints, the virtual IoT network constructed by the proposed method is able to achieve high scalability, low latency, and high communication efficiency at a relatively low cost.

Keywords

brain network; virtual network; Internet of Things (IoT); wireless sensor networks (WSN); exponential distance rule (EDR)

1. INTRODUCTION

Wireless sensor networks (WSNs) are ad-hoc type of networks on which wireless communication devices with sensor functionality connect to each other for gathering information

Permission to make digital or hard copies of all or part of this work for personal or classroom use is granted without fee provided that copies are not made or distributed for profit or commercial advantage and that copies bear this notice and the full citation on the first page. Copyrights for components of this work owned by others than ACM must be honored. Abstracting with credit is permitted. To copy otherwise, or republish, to post on servers or to redistribute to lists, requires prior specific permission and/or a fee. Request permissions from permissions@acm.org.

IMCOM '17, January 05-07, 2017, Beppu, Japan

© 2017 ACM. ISBN 978-1-4503-4888-1/17/01...\$15.00

DOI: <http://dx.doi.org/10.1145/3022227.3022304>

from the environment. With the recent progress in miniaturization of wireless devices and the increased sophistication in function, WSNs are expected to serve as the basic technology for the *Internet of Things* (IoT). In the future IoT scenario, the number of connected wireless devices is expected to increase drastically and the types of applications on those devices is going to diversify beyond the current role as WSNs. However, in the current IoT situation, individual networks are constructed according to each provider's policy and mainly transfer information through the Internet [8, 22].

Virtualization of WSNs has also received a lot of attention for the realization of IoT as a social infrastructure. Therefore, we consider in this paper a virtualized IoT network, which is composed of an infrastructure layer on which physical IoT resources are inter-connected and a service layer for communication networking. We assume that each IoT network is constructed based on its provider's policies to fulfill its purpose or specification of application service. In other words, this paper deals with the construction of a virtual IoT network topology by virtually interconnecting between these individual physical IoT networks as subnetworks or network modules. This virtual IoT network permits administrators on the service layer to provide the required function to each user. For the construction of the virtual IoT network, it is substantially important to reveal an appropriate and efficient way to connect between each module and create the network taking into account scalability, construction cost, and communication efficiency.

As an inspiration to solve this problem, we focus on recent results from the analysis of brain networks in neuroscience, which has progressed remarkably in recent years. Brain networks are well known for their high communication efficiency and low metabolic cost, i.e., the amount of consumed energy needed for performing a given task, and thus the characteristics of brain networks are very suitable to help in developing efficient telecommunication networks. In recent work, brain networks have been characterized by their small-world or scale-free properties [2, 5, 20].

This paper utilizes another novel brain network model with geometric constraints, the *Exponential Distance Rule* (EDR) model, which was proposed by Ercsey-Ravasz et al. [6, 15, 16]. The brain's cortex is composed of multiple areas

separated by their local functional roles. The EDR model describes the inter-areal connectivity structure, where multiple neural links are generated between pairs of brain areas according to a probability function that decays with distance between these areas. Comparison between cortical networks obtained from measurements and artificial networks generated by the EDR model revealed that the EDR model can generate networks with similar graph-topological features [6].

In this paper, we propose a construction method of a virtual IoT network based on the EDR model. We associate the areas in cortical networks with the networks of wireless devices (WSN modules) of different IoT networks, and neurons in each of those areas with wireless devices in the WSN modules. We assume that if the distance between base stations from any pair of modules is small enough, they can be interconnected. Over the infrastructure layer of inter-connected WSN modules, we construct virtual networks based on the EDR model and study the performance of the proposed virtual IoT network topologies.

The structure of this paper is as follows. In Section 2, we introduce related work on brain networks and *virtualized wireless sensor networks* (VWSNs). Then, we propose our novel method to construct VWSN based on the generative brain network model in Section 3. In Section 4, we show the results from simulations. Finally, we conclude our paper in Section 5.

2. RELATED WORK

In this section we will briefly introduce existing research in the two major areas that our paper is addressing: virtualization of wireless sensor networks and brain networks.

2.1 Virtualized Wireless Sensor Networks

WSNs are currently being integrated into IoT and virtualization of WSNs is attracting a lot of attention due to its benefits: (i) new application services can reuse existing network resources, (ii) heterogeneity between network units can be abstracted away to overcome differences between infrastructure modules, and (iii) the separation of application and infrastructure accelerates the development of new services [11, 13]. These features allow WSNs to become more flexible systems, and therefore virtualization is regarded as key technology to realize future IoT networks.

The architecture for a *Virtualized Wireless Sensor Network* (VWSN) is shown in Fig. 1, see [8]. In this architecture, *Sensor Infrastructure Providers* (SInPs) deploy many physical sensor network resources that form WSN modules. Above that, *Sensor Virtualization Network Service Providers* (SVNSPs) hire infrastructure resources from SInPs, and thus create *Virtualization of Sensor Network* (VSN).

Such an architecture is certainly effective for efficient utilization of resources and flexible network construction. However, it lacks some attention to the future IoT situation. The expected increase in application service variety will also cause frequent modifications, such as addition/removal of nodes or links, or construction/destruction of virtual networks. Even though the construction of virtual networks is easier than that of physical networks, it is still difficult to determine the network topology which is best for each application service. The rapidly increasing number of nodes leads to higher complexity in future WSNs to collect the latest information from the whole network. Therefore, com-

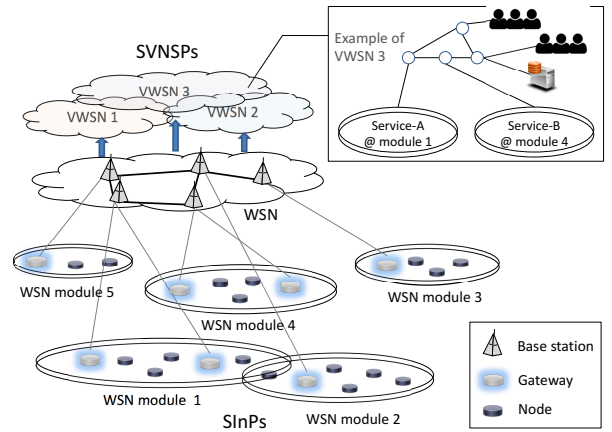


Figure 1: Virtualized wireless sensor networks composed of underlying physical networks

putational complexity and the cost for topology design will be too high for frequent construction.

2.2 Connectivity Structure of Brain Networks

The connectivity structure of brain networks has been recently studied from the viewpoint of complex networks and discussions on the structure has progressed with regard to the small-world or scale-free properties [2, 5, 19, 20]. Network models taking these properties into account can reproduce the high modularity and low hop-counts found in brain networks, but most models ignore the physical lengths of links. In a mammalian brain network, the metabolic cost to generate and maintain neural connections increases with the physical distance between neurons. On the other hand, for the quick information integration over the whole brain network, it is necessary to connect neurons that are far from each other. Ultimately, brain networks are constructed based on the trade-off between metabolic cost and communication efficiency [9]. Therefore, it is pointed out in [12] that the models without distance constraints cannot adequately reproduce the structural characteristics of brain networks.

In telecommunication networking, both wired and wireless networks have to reduce communication distances: in wired networks, the increase of link length directly causes an increase of wiring cost, whereas in wireless networks, distant communication requires high transmission power to overcome signal attenuation and interference. However, long connections are vital for information integration, suppression of communication delays, and robustness.

We focus on the similarity between brain and telecommunication networks regarding the relationship of efficiency and distance constraints, and apply these mechanisms to construct better topologies in terms of construction cost and communication efficiency.

3. PROPOSED VIRTUAL IOT TOPOLOGY CONSTRUCTION METHOD

3.1 Cortical Inter-Areal Connectivity Model

The *Exponential Distance Rule* (EDR) model is a network model which is derived from the anatomical connectivity structure of the macaque monkey [6]. For the construction

of the EDR model, Ercsey-Ravasz et al. used in [6] a parcellation of the entire macaque cortex into 91 cortical areas, i.e., areas consisting of similar types of neurons, and proposed a network graph whose nodes represent each cortical area. They picked 29 of the spatially distributed 91 cortical areas, so that the subgraph of these 29 areas can provide a complete estimation of the entire network. Retrograde tracer injections into those 29 areas revealed 6,494,974 neural connections and 1,615 inter-areal connections and that the existence probability $p(d)$ of neural connections exponentially decays with the inter-areal distance, see Eq. (1).

$$p(d) = c \exp(-\lambda d) \quad (1)$$

The term c is a normalization constant, d is the physical distance between areas, and λ is an intensity parameter ($\lambda = 0.180 \text{ mm}^{-1}$ used in [6] to approximate the cortical connectivity of macaques). Regarding the creation of neural links, physical distance becomes a very critical constraint since the establishment and maintenance of neural connectivity requires significant metabolic cost [9]. Therefore, neurons tend to form connections with other closer neurons and locally create dense clusters, while having very few long-distance connections to remote neurons to accelerate information integration. Equation (1) expresses the existence probability of a neural link with inter-areal distance d . Even though EDR is a very simple model with only a single parameter λ , it can reproduce various properties of cortical inter-areal networks, such as communication efficiency, distribution of cliques, eigenvector spectra, existence of core structure, etc. [6].

A similar graph model to EDR by Waxman [21] is sometimes used for modeling the Internet topology. However, while a vertex in the Waxman model represents a network node, it represents a module containing multiple nodes in EDR. The idea of constructing a topology among modules is the starting point of our proposed method. Unlike the Waxman model, which only runs a single trial on every vertex pair whether to form a link during construction of the binary graph, vertex pairs are repeatedly and randomly selected in EDR while creating weighted connections between vertices. Besides, only a single parameter is used for EDR, while a combination of two parameters is used in the Waxman model.

3.2 Construction of Virtual IoT Network

WSNs are considered as the basic technology for IoT [14, 23] and, in combination with network virtualization, they can construct flexible and efficient virtual IoT networks on distributed wireless network devices [8, 10]. In our model, we assume a network that consists of two layers: *Infrastructure Layer* (Infra-Layer) and *Virtualized Service Layer* (VS-Layer), see Fig. 2. We assume that the devices on Infra-layer are supplied as physical resources, where wireless network devices physically connect to each other and form network modules. Then, gateway nodes in Infra-Layer modules virtually connect to each other and form the VS-Layer. In this context, we assume that any node has the ability to serve as a gateway node and its role depends on whether it is connected to an Inter-VL or not.

We now propose a method to construct a network topology on VS-Layer in this virtual IoT network model. In our method, we slightly modify Eq. (1) from the EDR model that defines the probability of generating connections for the

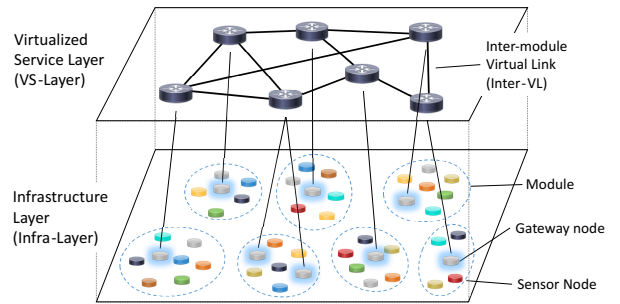


Figure 2: Virtual IoT network model

VS-Layer. The EDR model does not specify how nodes are connected by *Inter-module Virtual Links* (Inter-VLs), therefore we now describe the algorithm to construct the virtual IoT network model in our proposed method.

3.2.1 Infra-Layer

The Infra-Layer is composed of multiple WSN modules. When constructing the Infra-Layer, we first deploy N nodes randomly in the area and then connect all nodes located within a certain communication range r of each other. Next, we partition the network into modules with the InfoMap method [18]. Finally, we remove connections between modules and obtain the resulting topology at Infra-Layer.

3.2.2 VS-Layer

In the process of InfoMap module division, a gateway node is determined for each module, through which the flow of random walks between all node pairs in each module is maximal. We define the coordinate of this representative node as the coordinate of the module. Modules connect to each other via these representative nodes according to the probability function in the EDR model and form Inter-VLs. In this manner, the VS-Layer is constructed.

Regarding the formation of Inter-VLs, we modified the variable and parameters in Eq. (1) to the following Eq. (2) and generate Inter-VLs with probability $p(d_n)$ in order to widen the application range of the EDR model from cortical inter-areal connectivity to IoT.

$$p(d_n) = \exp(-d_n/\alpha) \quad (2)$$

In Eq. (2), d_n is the relative distance between two specific modules, i.e., $d_n = d/d_{max}$ where d is the actual Euclidian distance and d_{max} is the largest of all inter-module distances. To define a control parameter between 0 and 1 so that Eq. (2) becomes adaptive to any scale of networks, we replace λ by a new parameter $\alpha = (\lambda d_{max})^{-1}$. Thus $p(d_n)$ represents the probability whether to form a connection between these two modules. Since we repeat the procedure for generating Inter-VLs until a certain number of links is reached, we set the normalization constant $c = 1$ in Eq. (1).

In the construction of the VS-Layer, we repeat the formation of Inter-VLs according to the probability $p(d_n)$ between randomly chosen modules until we reach a predefined number of L Inter-VLs. At this time, $L = mM$, where M is the number of modules and m is a parameter that determines the density of Inter-VLs among all module pairs. As a characteristic of our proposed method, multiple Inter-VLs can be assigned between the same module pair. When we finish

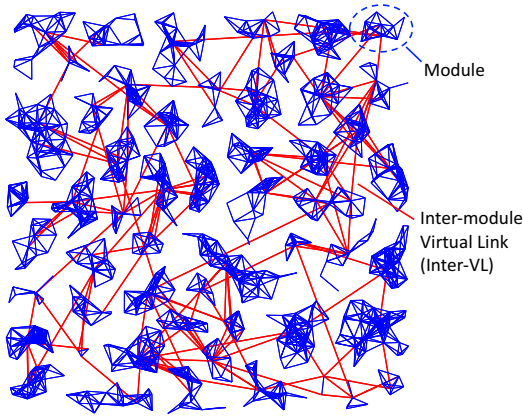


Figure 3: Inter-connected IoT network model

generating the VS-Layer, we next assign edges of Inter-VLs to nodes in the modules.

3.2.3 Assigning Endpoints of Inter-VLs

Inter-VLs are connected to nodes in modules at the Infra-Layer, passing through the VS-Layer. There are various ways to assign Inter-VL edges to nodes and in this paper we select them in the order of the node degrees. This means that endpoint nodes of Inter-VLs are chosen so that the sum of the degrees becomes highest among all possible pairs of endpoints. By this assignment, we exclude pairs of endpoints on which Inter-VLs already exist.

It is one of features of the EDR model that one or more links can connect two modules. We define the weight between two modules as the number of links between them. Figure 3 shows an example network as the outcome of the above procedure, where each link is unweighted and undirected.

4. SIMULATION RESULTS

In this section, we discuss the results from computer simulations to evaluate the performance of the virtual IoT network constructed by our proposed method.

4.1 Reference Network Topologies

We generate a virtual IoT network topology using Eq. (2), which is inspired by the EDR model. This equation can vary the ratio of inter-module links by adjusting the parameter α . In the following evaluation, we prepared several EDR networks with different α , as well as some reference network models: Random model, Barabási-Albert (BA) model, Full-Link model, and Minimum-Link model, which we will explain in the following subsections.

Random Model

For the construction of the Random model, we repeat randomly choosing a pair of modules and connecting them. This procedure stops when L Inter-VL are generated.

BA Model

The Barabási-Albert (BA) model [1] is one of the most well-studied complex network models that have the scale-free property and they are often used in the field of information networking to generate Internet-like topologies. When

constructing a topology based on the BA model, we first choose 5 modules and create an initial full-mesh topology. Then, we repeatedly add a new module to the initial topology, and at each time we probabilistically choose m' other modules from the existing topology for generating a connection between those modules. At this time, the probability that module i is chosen is given by $p_i = k_i / \sum_j k_j$, where k_i is the degree of the virtual node representing module i and m is chosen so that the same number of Inter-VLs are generated with the EDR model, and approximately $m' = m$.

Full-Link Model

The Full-Link model constructs a topology with links between all pairs of modules. As a result, this model is the most costly, but most efficient in terms of path length and hop count.

The Minimum-Link Model

The Minimum-Link model constructs a topology with the minimum total length of links having the same number of Inter-VLs as the other models except the Full-Link model. For the construction, we first generate a minimum spanning tree topology and then add links between the closest pair of modules until a sufficient number of Inter-VLs is generated. In contrast with the Full-Link model, this model realizes the smallest cost while communication efficiency is considerably low.

4.2 Evaluation Metrics

We will now describe the network metrics that will be used to compare the topologies.

Average Path Length (APL)

APL is a metric which calculates the average path length between all node pairs. In this context, the path length is the smallest sum of all link lengths on the route between a node pair. Each path is composed of two types of links: intra-module links from a node to a gateway node on Infra-Layer and inter-module links between gateways on VS-Layer.

Average Hop Count (AHC)

AHC is a metric which calculates the average hop count between all node pairs. Similar to APL, we also use here the route that minimizes hop counts between node pairs.

Wiring Cost (WC)

We determine WC to estimate the cost needed to construct a certain topology. Since we focus on wireless networks, WC is calculated as the sum of squares of the lengths of all Inter-VLs on VS-Layer based on the Friis transmission equation [7], which predicts that energy consumption on wireless signal transmission increases with the square of distance.

Modularity

Modularity is the metric that expresses the degree of community structure found in a network topology [17]. When we determine modularity, we divide a network into a partition of modules and modularity is expressed by the fraction of the edges that fall within the given groups minus the expected fraction if edges were distributed at random. The

calculation of modularity Q follows Eq. (3).

$$Q = \sum_i (e_{ii} - a_i^2) \quad (3)$$

In Eq. (3), e_{ij} is the proportion of links between modules i and j divided by the total number of all links and $a_i = \sum_j e_{ij}$. In other words, e_{ii} is the proportion of links within a module i to all links, a_i is the proportion for an endpoint of a certain link to be contained in a module i , and a_i^2 is the proportion for both edges of a certain link to be contained in module i . In our evaluation, we regard a single WSN module as a node in this equation, i.e., we evaluate modularity of topologies on VS-Layer. Then, we use InfoMap [18] to divide a VS-layer topology into modules for calculating Eq. (3).

Information Spreading Speed

In order to evaluate the efficiency of the virtual IoT network topologies for spreading information, we perform simulations of flooding and measure the time needed for data packets to spread over all nodes on each topology. Since it still remains unpredictable what type of traffic patterns will appear in future, we perform flooding in our simulation to measure the average time of information diffusion. When a data packet arrives at an arbitrary node, the node forwards this packet to each of its neighboring nodes. In this context, an adjacent node means that the nodes are connected by one hop on Infra-Layer or VS-Layer. When a node receives a packet, it drops the packet if it had previously received one in the past, otherwise it passes the packet to its neighbors. In this flooding simulation, two types of delay will occur: (i) the *service delay* on each node according to the exponential distribution with service rate $\mu = 1/D \text{ s}^{-1}$ and (ii) the *propagation delay* over each link which takes $D \text{ s}$ per 100 m. These two types of delay were selected in such way that the service delay on a node becomes on average equal to the propagation delay on a 100 m link. In this manner, we investigate the average time for a single packet to spread over the entire topology.

4.3 Evaluation Results

4.3.1 Structural Properties of Models

We compared the structural properties of the generated virtual IoT networks and summarized the results in Table 1. We assume a $300 \times 300 \text{ m}^2$ square area and deploy $N = 4,000$ nodes, each having $r = 8 \text{ m}$ communication range. The InfoMap algorithm generates $M = 223$ modules on average in all simulations. All models use a link density of $m = 5$ and all models except the Full-Link model have the same number of links $L = mM$. All values shown in Table 1 are the average results from 100 computer simulation runs.

Average Path Length (APL).

The Full-Link model minimizes APL, since it generates Inter-VLs between all possible pairs of modules, while the Min-Link model shows the worst score, since it specializes in reducing the cost by sacrificing efficiency. Remarkably, $\text{EDR}_{\alpha=0.025}$ has the second smallest APL, which is very close to that of the Full-Link model, where the EDR model generates numerous short Inter-VLs and only few long links to construct the VS-Layer. The long distance Inter-VLs contribute to a short APL because they are mostly included in the minimum paths between distant nodes. On the other

hand, the short Inter-VLs contribute to decreasing the possibility of making detours on the topologies. From the result of $\text{EDR}_{\alpha=0.025}$, we can tell that the proportion of long to short Inter-VLs makes the parameter $\text{EDR}_{\alpha=0.025}$ decrease APL. We will provide further investigation on the effect of this parameter α in Section 4.3.3.

As we increase the value of α in EDR, the proportion of long Inter-VLs increases and its topological shape approaches that of the Random model where the lack of short links causes detours between pairs of nodes and therefore APL increases. The BA model ignores the geometric features when constructing a topology and its APL becomes almost the same as that of the Random model.

Average Hop Count (AHC).

For the same reason as APL, the Full-Link model has the highest decrease for AHC and the Min-Link model visibly increased its AHC, rendering the topology no longer usable. The model which showed the second smallest value was the BA model. This is the effect of the existence of hub nodes in the BA model, which is the unique feature of this model. By passing through these hub nodes, the BA model can decrease hop counts among nodes. Meanwhile, $\text{EDR}_{\alpha=0.025}$ showed the largest AHC value except for the Min-Link model. This is because it has the smallest number of long Inter-VLs and, therefore, in order to reach a certain node, the route has to be composed of many short Inter-VLs.

Wiring Cost (WC).

The Min-Link model creates a connected topology with the possible minimum WC forming L Inter-VLs. Note that the Full-link model generates Inter-VLs between all module pairs and results in generating a ${}_M C_2 / mM \approx 22.3$ times larger number of Inter-VLs than other models. On the other hand, $\text{EDR}_{\alpha=0.025}$ has a much smaller value compared to the others except for the Min-Link model, having 0.027 times for the Random model and 0.0012 times for the Full-Link model. From these results, we can definitely say that $\text{EDR}_{\alpha=0.025}$ can considerably decrease the wiring cost of a topology approaching to the Min-Link model. The Random and BA models ignore geometric constraints as we mentioned in the APL paragraph and their WC is higher than the other models except for the Full-Link model.

Modularity.

The Full-Link model appears to be here a special case, since maximum modularity of 1.0 is reached by having the whole network as a single large module. $\text{EDR}_{\alpha=0.025}$ showed the second largest value. This may be since $\text{EDR}_{\alpha=0.025}$ locally generates many dense topological structures by numerous short Inter-VLs and a few long Inter-VLs connecting that local structure. In this manner, $\text{EDR}_{\alpha=0.025}$ can create high modularity. Compared to the Random model, the BA model showed a slightly lower value. This is because the BA model creates a topology that can be separated into a core and periphery [3, 4], and therefore the resulting topology lacks a homogeneous community structure.

4.3.2 Differences Between Network Sizes

We next investigate the effect of the different network models on the number of modules in the virtual IoT network. Previously, we deployed $N = 4,000$ nodes on a $300 \times 300 \text{ m}^2$ square area. In addition to the results discussed above, we

Table 1: Comparison of structural properties between network models ($N = 4,000$)

	Min-Link	EDR $_{\alpha=0.025}$	EDR $_{\alpha=0.10}$	EDR $_{\alpha=0.40}$	Random	BA	Full-Link
APL [m]	504	193	197	247	297	296	171
AHC	35.3	9.53	7.01	6.86	6.91	6.57	4.15
WC [$10^5 m^2$]	0.00594	0.0583	0.492	1.51	2.19	2.17	47.6
Modularity	0.365	0.690	0.426	0.285	0.285	0.255	1.00

also evaluated the same metrics as in Section 4.3.1, where $N = 8,000$ nodes are deployed on a $300\sqrt{2} \times 300\sqrt{2} m^2$ square area, while keeping all other settings the same, see Table 2. When $N = 4,000$, the number of modules is $M \approx 223$, whereas for $N = 8,000$ the number of modules becomes $M \approx 422$ on average for 100 repetitions of the computer simulation. Additionally, we calculated the ratios of the values in Table 2 divided by those in Table 1, as shown in Table 3, in order to see the change in performance for each model when it scales larger or smaller in terms of the number of modules.

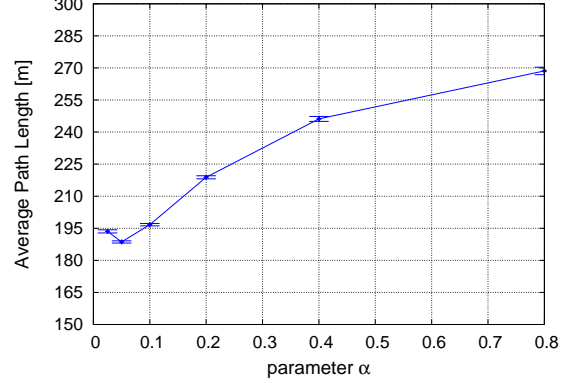
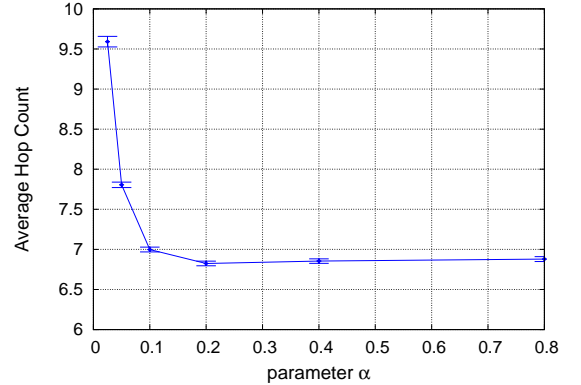
According to Table 3, AHC and modularity show almost no difference, but APL and WC show remarkable features. Regarding APL and WC metrics, EDR $_{\alpha=0.025}$ showed the lowest values of all models. Thus, when constructing topologies with a larger number of modules, EDR $_{\alpha=0.025}$ can keep APL and WC smaller than the other models, while AHC does not increase at all. We can attribute this to the high modularity of EDR $_{\alpha=0.025}$, because a higher community structure enables the topology to easily shift to a larger scale. The Full-Link model has the highest modularity among all models. However, it lacks sparseness and plasticity, and therefore it cannot adapt to a larger scale. Another important finding is that although the Min-Link keeps WC the smallest when the network becomes larger, AHC and APL become much worse and lose their community structure.

4.3.3 Trade-off for Cost and Efficiency over α

In Sections 4.3.1 and 4.3.2, we revealed novel characteristics of the virtual IoT network topology based on the EDR model with small parameter α . Therefore, in this Section 4.3.3 we focus only on the EDR model and observe the effect of its parameter α . Figures 4–6 show APL, AHC, and WC, respectively, for $N = 4,000$ on the y-axis, and the x-axis represents α . The results are averaged over 50 simulation trials and error bars show confidence intervals for the 95% confidence level.

Among the three figures, only APL shows non-monotonic characteristics as seen in Fig. 4. We already mentioned in Section 4.3.1 the importance of the proportion of long and short Inter-VLs which depends on the parameter α . From Fig. 4, it can be said that if α is increased, APL increases due to the detour on routes between nodes, and at the same time if α decreases too much, APL increases again because of the lack of shortcuts between distant nodes. Therefore, the best parameter for reducing APL is about $\alpha = 0.05$, which provides the best proportion of long and short Inter-VLs.

Observing Fig. 5, we can easily find that AHC does not change much in the range of $0.1 \leq \alpha \leq 0.8$ and drastically increases as the parameter α is smaller than 0.1. From this result, we can conclude that the lack of long Inter-VL does not have much influence on AHC in the range of $\alpha \geq 0.1$ and below this value, the topology lacks long Inter-VLs and distant areas become difficult to reach, leading to an increase

**Figure 4: Average Path Length over α** **Figure 5: Average Hop Count over α**

of AHC. Figure 6 tells us the most basic tendency of the topology: as we decrease the parameter α , WC exponentially decays, reflecting the exponential feature of Eq. (2).

As we have shown above, there is a trade-off between cost and efficiency depending on the parameter α : APL keeps the lowest value around $0.025 \leq \alpha \leq 0.10$, while AHC and WC show drastic increase and decrease as α approaches 0. Therefore, in summary, we can conclude that our proposed method can create a topology that satisfies the best performance of cost and efficiency for each user by only adjusting the parameter α at around 0.05.

4.3.4 The Effect of Weight Assignment on Information Spreading Speed

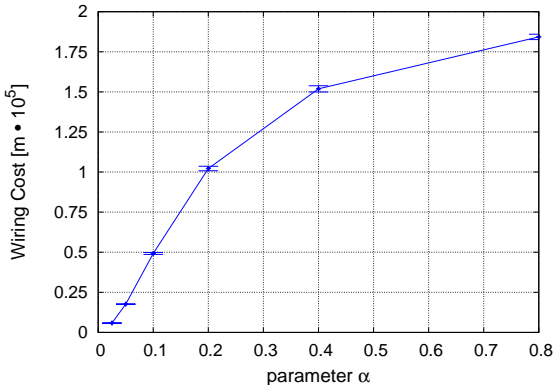
In the previous section, we have shown that our proposed method performs best with the parameter $\alpha \approx 0.05$. Thus, we set this parameter fixed to 0.05 and investigate the effect of the weight assignment by the EDR model. A small α is also preferable to study this effect, since multiple Inter-VLs

Table 2: Comparison on structural properties between models ($N = 8,000$)

	Min-Link	EDR $_{\alpha=0.025}$	EDR $_{\alpha=0.10}$	EDR $_{\alpha=0.40}$	Random	BA	Full-Link
APL [m]	793	250	276	361	454	436	236
AHC	54.6	10.5	7.72	7.66	7.64	7.24	4.29
WC [10^5m^2]	0.00815	0.133	1.28	3.92	5.70	5.71	228
Modularity	0.337	0.701	0.429	0.292	0.291	0.247	1.00

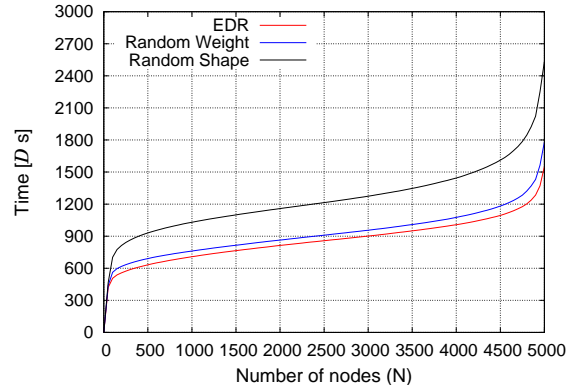
Table 3: Ratio of properties small to large scale of networks (Table 2/Table 1)

	Min-Link	EDR $_{\alpha=0.025}$	EDR $_{\alpha=0.10}$	EDR $_{\alpha=0.40}$	Random	BA	Full-Link
APL	1.57	1.29	1.40	1.45	1.52	1.47	1.38
AHC	1.54	1.11	1.10	1.12	1.10	1.10	1.03
WC	1.37	2.28	2.59	2.58	2.60	2.63	4.78
Modularity	0.92	1.02	1.00	1.02	1.02	0.96	1.00

**Figure 6: Wiring Cost over α**

are easily found in nearby modules. In this context, weight corresponds to the number of Inter-VLs between modules and the EDR model creates a topology where the weight becomes larger as the distance between the modules becomes smaller. For comparison, we also prepare two types of randomized models with the same wiring cost.

The first is the *Random Weight* model, where we randomly reassign the weights between the modules while keeping the total lengths of Inter-VLs. At this time, we do not generate Inter-VLs between modules if they aren't connected among each other by Inter-VLs. The other model is the *Random Shape* model, where we generate a random VS-Layer topology that has the same total length of Inter-VLs as the original EDR model. Rather than keeping the number of Inter-VLs fixed, we believe it is more important to keep the total wiring cost constant in this evaluation because it shows the performance difference at the same construction cost. If we ignore this cost, the rewired topology has much higher cost and efficiency at the same time and is not suitable for comparison. For the evaluation of the effect of the weight assignment, we run a flooding simulation and evaluate the information spreading speed. Each topology has $N = 5,000$ nodes on a $200 \times 200\text{m}^2$ area and divided into $M \approx 102$ modules by InfoMap on average. We used $m = 25$ so that the effect of weight assignment becomes clearer. The communication range of each node is $r = 8\text{m}$ and is the same value as in the previous evaluation. We run the simulation on 20 topologies and for 10 packet flows on each topology.

**Figure 7: Information spreading speed on models of different Inter-VL assignments**

The result is shown in Fig. 7, where the x-axis represents the number of nodes N over which a data packet is spread and the y-axis represents the time it takes to spread over N nodes.

Figure 7 shows that the *Random Shape* model spreads data packets slowest among the three methods. This implies that the topological shape of the EDR model is reasonable for efficient information spreading. The more interesting and notable point is that the original EDR model is superior to the *Random Weight* model. This means that generating many Inter-VLs between nearby modules is preferable for quick information spreading over costly long Inter-VLs between distant modules. From those results, we can say that the weight assignment method of the EDR model is efficient in terms of information spreading and, therefore, our proposed method can provide a high performance when parameter α is adjusted to a small value around 0.05 and applied to a network where each module consists of a large number of nodes.

5. CONCLUSION

In this paper, we proposed and evaluated a method to construct a virtual IoT network that has similar structural features as the brain's cortical network. For $\alpha \approx 0.05$, the generated network showed a good performance in the trade-off between cost and efficiency. Furthermore, our method did not degrade its performance in comparison with other

models when the number of modules became larger. Besides, when the number of sensor nodes in each module increase, the unique weight assignment of EDR produced a better performance than other methods. Now we can conclude that our proposed brain-inspired method can produce a virtual IoT network topology, which utilizes features that originate from brain networks with the best performance in the trade-off between cost and efficiency, as well as high scalability. Furthermore, our proposed method will bring more benefits when we apply the method to the future IoT situation, whose traffic pattern is considered to require modules in close proximity to communicate and cooperate with each other.

However, in this paper we only considered structural properties. We can further improve our method by including other constraints when constructing a topology for a better community structure. For example, the BA model showed better evaluation in AHC over $EDR_{\alpha=0.025}$ and, therefore, a combination with the preferential attachment method may improve our method.

Besides, performance limitations of sensor nodes are so far unconsidered in our method. For a more realistic situation, the upper limit of processing performance of a node has to be considered. In relation to that, we need to define how our method can share the same node among different application services when multiple VS-Layers are constructed. Further evaluations with more strict simulation settings are necessary to investigate these issues.

6. ACKNOWLEDGMENTS

This research was supported by “Program for Leading Graduate Schools” of the Ministry of Education, Culture, Sports, Science and Technology, Japan, and a Grant-in-Aid for Scientific Research (A) (No. JP15H01682) from the Japan Society for the Promotion of Science (JSPS), Japan.

7. REFERENCES

- [1] A.-L. Barabási and R. Albert. Emergence of scaling in random networks. *Science*, 286(5439):509–512, 1999.
- [2] D. S. Bassett and E. Bullmore. Small-world brain networks. *The neuroscientist*, 12(6):512–523, 2006.
- [3] S. P. Borgatti and M. G. Everett. Models of core/periphery structures. *Social networks*, 21(4):375–395, 2000.
- [4] P. Csermely, A. London, L.-Y. Wu, and B. Uzzi. Structure and dynamics of core/periphery networks. *Journal of Complex Networks*, 1(2):93–123, 2013.
- [5] V. M. Eguiluz, D. R. Chialvo, G. A. Cecchi, M. Baliki, and A. V. Apkarian. Scale-free brain functional networks. *Physical review letters*, 94(1):018102, 2005.
- [6] M. Ercsey-Ravasz, N. T. Markov, C. Lamy, D. C. Van Essen, K. Knoblauch, Z. Toroczkai, and H. Kennedy. A predictive network model of cerebral cortical connectivity based on a distance rule. *Neuron*, 80(1):184–197, Oct. 2013.
- [7] H. T. Friis. A note on a simple transmission formula. *Proceedings of the Institute of Radio Engineers*, 34(5):254–256, May 1946.
- [8] M. M. Islam, M. M. Hassan, G.-W. Lee, and E.-N. Huh. A survey on virtualization of wireless sensor networks. *Sensors*, 12(2):2175–2207, 2012.
- [9] M. Kaiser and C. C. Hilgetag. Nonoptimal component placement, but short processing paths, due to long-distance projections in neural systems. *PLoS Comput Biol*, 2(7):e95, 2006.
- [10] I. Khan, F. Belqasmi, R. Glitho, and N. Crespi. A multi-layer architecture for wireless sensor network virtualization. In *Wireless and Mobile Networking Conference (WMNC), 2013 6th Joint IFIP*, pages 1–4. IEEE, 2013.
- [11] I. Khan, F. Belqasmi, R. Glitho, N. Crespi, M. Morrow, and P. Polakos. Wireless sensor network virtualization: A survey. *IEEE Communications Surveys & Tutorials*, 18(1):553–576, 2015.
- [12] K. Knoblauch, M. Ercsey-Ravasz, H. Kennedy, and Z. Toroczkai. The brain in space. In *Micro-, meso-and macro-connectomics of the brain*, pages 45–74. Springer, 2016.
- [13] W. Li, F. C. Delicato, P. F. Pires, Y. C. Lee, A. Y. Zomaya, C. Miceli, and L. Pirmez. Efficient allocation of resources in multiple heterogeneous wireless sensor networks. *Journal of Parallel and Distributed Computing*, 74(1):1775–1788, 2014.
- [14] L. Mainetti, L. Patrono, and A. Vilei. Evolution of wireless sensor networks towards the internet of things: A survey. In *Software, Telecommunications and Computer Networks (SoftCOM), 2011 19th International Conference on*, pages 1–6. IEEE, 2011.
- [15] N. Markov, M. Ercsey-Ravasz, A. R. Gomes, C. Lamy, L. Magrou, J. Vezoli, P. Misery, A. Falchier, R. Quilodran, M. Gariel, et al. A weighted and directed interareal connectivity matrix for macaque cerebral cortex. *Cerebral Cortex*, page bhs270, 2012.
- [16] N. T. Markov, M. Ercsey-Ravasz, C. Lamy, A. R. R. Gomes, L. Magrou, P. Misery, P. Giroud, P. Barone, C. Dehay, Z. Toroczkai, et al. The role of long-range connections on the specificity of the macaque interareal cortical network. *Proceedings of the National Academy of Sciences*, 110(13):5187–5192, 2013.
- [17] M. E. Newman and M. Girvan. Finding and evaluating community structure in networks. *Physical review E*, 69(2):026113, 2004.
- [18] M. Rosvall and C. T. Bergstrom. Maps of random walks on complex networks reveal community structure. *Proceedings of the National Academy of Sciences*, 105(4):1118–1123, 2008.
- [19] O. Sporns. *Networks of the Brain*. The MIT Press, 1st edition, 2010.
- [20] M. P. van den Heuvel, C. J. Stam, M. Boersma, and H. H. Pol. Small-world and scale-free organization of voxel-based resting-state functional connectivity in the human brain. *Neuroimage*, 43(3):528–539, 2008.
- [21] B. M. Waxman. Routing of multipoint connections. *Selected Areas in Communications, IEEE Journal on*, 6(9):1617–1622, 1988.
- [22] A. Whitmore, A. Agarwal, and L. Da Xu. The internet of things—a survey of topics and trends. *Information Systems Frontiers*, 17(2):261–274, 2015.
- [23] A. Zanella, N. Bui, A. Castellani, L. Vangelista, and M. Zorzi. Internet of things for smart cities. *IEEE Internet of Things Journal*, 1(1):22–32, 2014.